

Homeostatic Mechanisms for Iron Storage Revealed by Genetic Manipulations and Live Imaging of *Drosophila* Ferritin

Fanis Missirlis,^{*,1} Stylianos Kosmidis,[†] Tom Brody,[‡] Manos Mavrikakis,^{*} Sara Holmberg,^{*} Ward F. Odenwald,[‡] Efthimios M. C. Skoulakis[†] and Tracey A. Rouault^{*}

^{*}Cell Biology and Metabolism Branch, National Institute of Child Health and Human Development, Bethesda, Maryland 20892,

[†]Institute of Molecular Biology and Genetics BSRC "Alexander Fleming," Vari, 16672, Greece and

[‡]Neural Cell-Fate Determinants Section, National Institute of Neurological Disorders and Stroke, Bethesda, Maryland 20892

Manuscript received April 28, 2007

Accepted for publication June 22, 2007

ABSTRACT

Ferritin is a symmetric, 24-subunit iron-storage complex assembled of H and L chains. It is found in bacteria, plants, and animals and in two classes of mutations in the human L-chain gene, resulting in hereditary hyperferritinemia cataract syndrome or in neuroferritinopathy. Here, we examined systemic and cellular ferritin regulation and trafficking in the model organism *Drosophila melanogaster*. We showed that ferritin H and L transcripts are coexpressed during embryogenesis and that both subunits are essential for embryonic development. Ferritin overexpression impaired the survival of iron-deprived flies. *In vivo* expression of GFP-tagged holoferritin confirmed that iron-loaded ferritin molecules traffic through the Golgi organelle and are secreted into hemolymph. A constant ratio of ferritin H and L subunits, secured via tight post-transcriptional regulation, is characteristic of the secreted ferritin in flies. Differential cellular expression, conserved post-transcriptional regulation via the iron regulatory element, and distinct subcellular localization of the ferritin subunits prior to the assembly of holoferritin are all important steps mediating iron homeostasis. Our study revealed both conserved features and insect-specific adaptations of ferritin nanocages and provides novel imaging possibilities for their *in vivo* characterization.

IRON is an essential element of aerobic life. Cells have evolved highly regulated molecular pathways that ensure iron incorporation into heme (PONKA 1997) or formation of iron-sulfur clusters (ROUAULT and TONG 2005). Cellular and systemic iron levels are tightly regulated to ensure bioavailability and protect from the hazards of iron overload (HENTZE *et al.* 2004). Ferritin, a heteropolymer composed of H and L subunits, acts as the primary iron-storage molecule (HARRISON and AROSIO 1996). The H subunit contains a ferroxidase center, which enables the mature heteropolymer to oxidize soluble ferrous iron, whereas the L chain provides the nucleation centers for deposition of the ferrihydrite mineral (SANTAMBROGIO *et al.* 1996).

In mammals, transcriptional control of the ferritin genes influences the relative ratio of H to L chains in different cell types (TORTI and TORTI 2002; PHAM *et al.* 2004). Translation of ferritin proteins is regulated by the binding of either of the two iron regulatory proteins (IRPs) to an iron responsive element (IRE) located on the 5'-untranslated region (UTR) of the respective mRNAs (PANTOPOULOS 2004; ROUAULT 2006). Hered-

itary hyperferritinemia cataract syndrome, a disease in which ferritin L-chain IRE mutations interfere with appropriate translational repression, illustrates the physiological importance of the IRP/IRE system (CAZZOLA 2002; ROUAULT 2006). Moreover, adult mice lacking IRP2 overexpress ferritin and develop variable degrees of late-onset neurodegeneration (LAVAUTE *et al.* 2001; SMITH *et al.* 2004; GALY *et al.* 2006) and anemia (COOPERMAN *et al.* 2005; GALY *et al.* 2005). Negative consequences of chronic ferritin H-chain overexpression have been verified in aging mice (KAUR *et al.* 2006). Conversely, protection from oxidative stress has been shown in young mice that overexpress ferritin H-chain, because of the iron-chelating properties of ferritin (KAUR *et al.* 2003; WILKINSON *et al.* 2006). A complete null for ferritin H-chain has been generated in mice; homozygous animals die *in utero*, whereas heterozygotes exhibit signs of mild iron deficiency (THOMPSON *et al.* 2003). Finally, mutations in the human ferritin L-chain lead to neurodegeneration in a condition described as neuroferritinopathy (LEVI *et al.* 2005). Altogether, these results underscore the importance of ferritin regulation in mammalian health.

In *Drosophila*, *Ferritin 1 heavy chain homolog* (*Fer1HCH*) and *Ferritin 2 light chain homolog* (*Fer2LCH*) encode the ferritin subunits that compose the major,

¹Corresponding author: National Institutes of Health, Bldg. 18T, Room 101, 9000 Rockville Pike, Bethesda, MD 20892.
E-mail: missirlf@mail.nih.gov

secreted form of ferritin (CHARLESWORTH *et al.* 1997; GEORGIEVA *et al.* 1999, 2002). The crystal structure of secreted ferritin from *Trichoplusia ni* revealed a symmetrical arrangement of H and L chains (HAMBURGER *et al.* 2005). Inter- and intrasubunit disulfide bonds were shown to be important for the folding/assembly of *T. ni* ferritin, and the respective cysteine residues mediating these bonds were also conserved in *Drosophila melanogaster*, suggesting that the ferritins of the two species share the same mode of assembly (HAMBURGER *et al.* 2005). The Fer1HCH amino acid residues that are required for ferroxidase activity in mammals were conserved in the insect ferritin structure, and a predicted Fer2LCH ferrihydrite nucleation site formed by the L-chains was also found (HAMBURGER *et al.* 2005).

As in vertebrates, the IRE/IRP system functions in *Drosophila* (ROTHENBERGER *et al.* 1990; MISSIRLIS *et al.* 2003). A functional IRE is present in the 5'-UTR of the *Fer1HCH* mRNA, but only in certain splice variants that are preferentially encoded under iron-limiting conditions (LIND *et al.* 1998; GEORGIEVA *et al.* 1999). In contrast, no IRE is present in *Fer2LCH* mRNA (GEORGIEVA *et al.* 2002). IRP homologs are expressed in the fly (MUCKENTHALER *et al.* 1998), and one homolog (IRP-1A) has been shown to bind to IREs from both *Drosophila* and mammals (LIND *et al.* 2006).

Intracellular localization of ferritin in many insects also differs from mammals. Ultrastructural studies, combining electron microscopy and energy electron-loss spectroscopy, have revealed the presence of Calpodes ferritin in intracellular membrane compartments (LOCKE and LEUNG 1984). *Drosophila* Fer1HCH and Fer2LCH subunits contain signal peptides that direct them to the endoplasmic reticulum upon translation. Fer1HCH also contains a predicted N-glycosylation site (NICHOL *et al.* 2002). The two subunits are predominantly expressed in the midgut and are also abundant in hemolymph, where ferritin may transport iron for nutritional needs of *Drosophila* tissues (GEORGIEVA *et al.* 2002).

This article shows that mutational inactivation of either *Fer1HCH* or *Fer2LCH* in *Drosophila*, as well as the disruption of the ferroxidase center of Fer1HCH, results in developmental arrest and fly embryonic lethality. We characterize a novel fly strain expressing GFP-tagged Fer1HCH and show that GFP-Fer1HCH is incorporated into endogenous functional ferritin. We use this strain to study induction and trafficking of ferritin in the fly midgut, the major iron-storing organ in the insect.

MATERIALS AND METHODS

***D. melanogaster* stocks:** Fly strain *Fer1HCH*^{G188}/*TM3* was sent to us by Lynn Cooley and is available at <http://flytrap.med.yale.edu> (KELSO *et al.* 2004). This line was generated from a screen utilizing a mobile exon encoding GFP carried in a

P-transposable element (MORIN *et al.* 2001), which landed in the second intron of the *Fer1HCH* gene (Figure 2A). *Fer1HCH*^{G188}/*TM3*, *Sb*, *ry* and *Fer2LCH*^{G25}/*TM3*, *Sb*, *ry* were generated during a large-scale mutagenesis screen (SPRADLING *et al.* 1999) and were obtained from the Bloomington *Drosophila* Stock Center (Indiana University) (nos.11497 and 11483, respectively). To generate *UAS-Fer1HCH* and *UAS-Fer2LCH* flies, expressed sequence tags LD03437 and LD01936 were obtained from the Berkeley *Drosophila* Genome Project and subcloned into pUAST. Clone LD03437 contains the *Fer1HCH* IRE, but we have omitted it from the transgenic construct using a downstream *Xho*I restriction site present within the 5'-UTR for cloning. To generate ferroxidase-inactive *UAS-Fer1HCH*^{*} we have mutated E₈₇ to K₈₇ and H₉₀ to G₉₀ (COZZI *et al.* 2000). The resulting plasmids were verified by sequencing and injected into embryos using conventional techniques (RUBIN and SPRADLING 1982). Overexpression was accomplished by means of the UAS/Gal4 binary expression system (BRAND and PERRIMON 1993). All phenotypes reported were confirmed with independent transgene insertions and we generated recombinant chromosomes (on the X and the third) carrying both *UAS-Fer1HCH* and *UAS-Fer2LCH*. Levels of ferritin expression were assessed by Western blotting and were found increasingly elevated in the following genotypes: (1) induction from the third chromosome recombinant +/+; *Actin-Gal4*/+; *UAS-Fer1HCH*, *UAS-Fer2LCH*/+; (2) induction from the X chromosome recombinant *UAS-Fer1HCH*, *UAS-Fer2LCH*/+; *Actin-Gal4*/+; +/+; and (3) induction from the X and third chromosomes *UAS-Fer1HCH*, *UAS-Fer2LCH*/+; *Actin-Gal4*/+; *UAS-Fer1HCH*, *UAS-Fer2LCH*/+.

Biochemical assays and RNA *in situ* hybridization: Antibodies, separation of proteins by SDS-PAGE, and Western blots (for reducing conditions, we add β-mercaptoethanol, boil the samples for 10 min, and separate on 12% acrylamide; for nonreducing conditions, we omit β-mercaptoethanol and do not heat the samples prior to separating on 6% acrylamide), as well as the assay for *in vivo* loading of ferritin with ⁵⁵FeCl₃, were all performed in triplicates as described before (MISSIRLIS *et al.* 2006). Methods for mRNA localization and photographic imaging are also provided in a previous publication (BRODY *et al.* 2002).

Prussian blue staining and immunohistochemistry: Midguts from larvae were dissected in PBS and quickly transferred to 4% formaldehyde in PBS for 30 min. Following washes with PBS, the tissue was permeabilized by treating with 1% Tween in PBS for 15 min. For detection of ferric iron, the samples were incubated in the dark with Prussian blue stain [2% K₃Fe(CN)₆, 2% HCl] for 45 min. Five washes with water followed and the preparations were mounted in water on glass slides (mounting in PBS will result in loss of the blue stain due to the change in pH) and imaged on a Nikon microscope (see below). For immunohistochemistry, we used the primary antibodies mouse anti-GFP (1:1000) from Molecular Probes (Eugene, OR) (A-11120) in combination with rabbit anti-Lava lamp (1:250) (a gift from John Sisson; Sisson *et al.* 2000) or rabbit anti-Fer2LCH (1:500) (MISSIRLIS *et al.* 2006), followed by secondary fluorescent antibodies Alexa Fluor 488-conjugated goat anti-mouse (1:1000) from Molecular Probes (A-11029) and Alexa Fluor 546-conjugated goat anti-rabbit (1:1000) from Molecular Probes (A-11035). Preparations were mounted on slides with Fluoromount-G (Southern Biotechnology Associates, Birmingham, AL) in preparation for microscopy.

Imaging: Images of GFP-ferritin in freshly dissected intestines mounted in PBS were captured using a Nikon ECLIPSE E600 microscope linked to a Nikon digital camera DXM1200F and were further processed by ACT-1, the application program for the DXM1200F digital camera and Adobe Photoshop. GFP was visualized using a Nikon mercury lamp and the B-2E/C

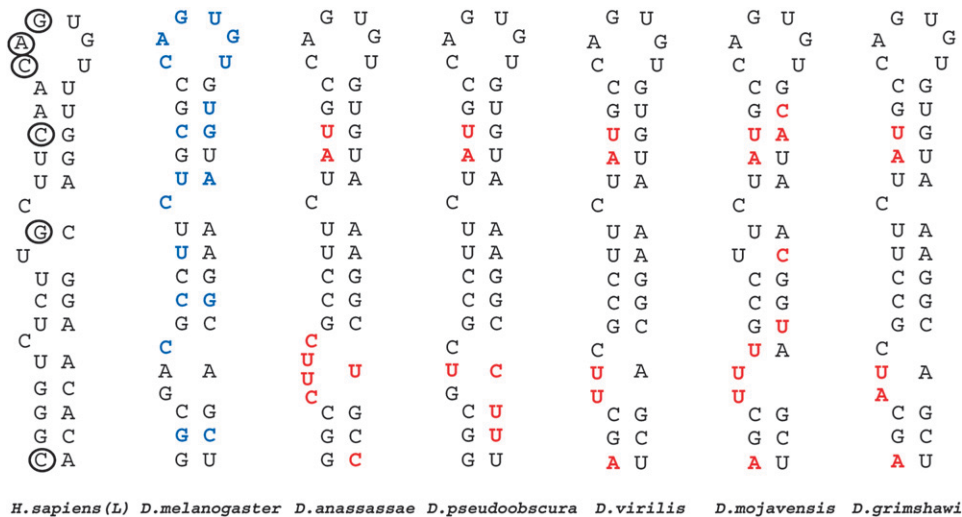


FIGURE 1.—Comparison of *Drosophila melanogaster Fer1HCH* IRE to human L-chain ferritin IRE and to *Fer1HCH* IREs from different *Drosophila* species. The IRE-containing alternative exon of *Fer1HCH* was conserved in all sequenced *Drosophila* species. Secondary structures from evolutionary divergent species of the *Drosophila* genus are compared to the *D. melanogaster* prototype. Nonconserved nucleotides are red. *D. melanogaster Fer1HCH* IRE was also compared to human L-chain ferritin IRE. Circled nucleotides are mutated in human disease (CAZZOLA 2002; ROUAULT 2006). Nucleotides conserved from human to *Drosophila* are blue.

FITC filter. Confocal microscope images of dissected tissues were captured with a 40 \times /1.2 NA water objective on a Zeiss 510 Meta inverted microscope using the 488-nm line of an argon laser with a 505–550 emission filter for GFP and the 543-nm helium-neon laser line with a 560–615 emission filter for Alexa Fluor 546-conjugated antibodies.

RESULTS

Conservation of the IRE in the *Drosophila* genus:

Two types of mutations in the IRE of the human L-ferritin gene cause hereditary hyperferritinemia cataract syndrome: mutations that disrupt base pairing of the stem loop and mutations that directly affect the specific CAGUG sequence of the loop and the cytosine of the IRE bulge (CAZZOLA 2002; ROUAULT 2006). The mutations that cause disease are detrimental to the defining features of IREs that are conserved from humans to flies (Figure 1). A survey of many sequenced *Drosophila* species confirmed that *Fer2LCH* mRNAs lack IREs, which are present only in the 5'-UTR of *Fer1HCH* transcripts. Comparison of the new IREs identified several nonconserved nucleotides between species, but in all cases the overall structure of the stem loop remained intact and the nucleotides implicated in disease were conserved or altered in ways that were compatible with base pairing (Figure 1). Considering the finding that *Fer2LCH* mRNA lacks the IRE and is not predictably regulated by IRP-1A, we asked whether other post-transcriptional control mechanisms govern *Fer2LCH* expression.

Characterization of P-element mutants in the ferritin genes: To study post-transcriptional regulation of *Fer1HCH* and *Fer2LCH* in *Drosophila*, we utilized flies with P-element insertions in these genes. We focused on three P elements: *Fer1HCH*⁴⁵¹ and *Fer2LCH*³⁵, which result in a loss-of-function mutant for each of the respective ferritin chains, and *Fer1HCH*^{G188}, which adds GFP to the H subunit (Figure 2A). *Fer2LCH*³⁵ is predicted to

cause a genetic null mutation because the transposable element disrupts the open reading frame, whereas in *Fer1HCH*⁴⁵¹ the P element resides in intronic sequences and the mechanism by which it disrupts gene function is unknown (Figure 2A). When homozygous, these insertions are embryonic or first instar larval lethal. Each insertion present over a deficiency chromosome lacking both genes also resulted in embryonic lethality, indicating that both ferritin-subunit chains perform essential functions in *Drosophila*.

To investigate possible homeostatic interactions between the two proteins, their expression in heterozygous adult flies was examined by Western blot analysis (Figure 2B). As expected, *Fer1HCH* levels were markedly reduced in *Fer1HCH*^{451/+} heterozygotes and the same was true for *Fer2LCH* levels in *Fer2LCH*^{35/+} flies. Unexpectedly, endogenous levels of *Fer2LCH* were also low in *Fer1HCH*^{451/+}, and *Fer1HCH* levels were low in *Fer2LCH*^{35/+} flies. Because *trans*-heterozygous (*Fer1HCH*⁴⁵¹/*Fer2LCH*³⁵) flies are fully viable, we hypothesized that neither of these insertions would directly affect the transcriptional activity of both genes simultaneously. To address the potential role of the P-element insertions on transcription at the locus, we ubiquitously overexpressed *Fer1HCH* in *Fer1HCH*^{451/451} homozygous flies and restored adult viability (Figure 2C; see also MATERIALS AND METHODS). When *Fer1HCH* was overexpressed in homozygous *Fer2LCH*^{35/35} flies, viability was not restored. The converse was true for overexpression of *Fer2LCH* (Figure 2C). These results indicate that the respective P elements interfere specifically with *Fer1HCH* and *Fer2LCH* expression and that reduction in levels of the alternate chain in each mutant is most likely due to post-transcriptional regulation.

We also generated flies that express *Fer1HCH* with a mutation that inactivates the ferroxidase activity, on the basis of analogy to the ferroxidase-null human allele (COZZI *et al.* 2000). Expression of the mutated transgene

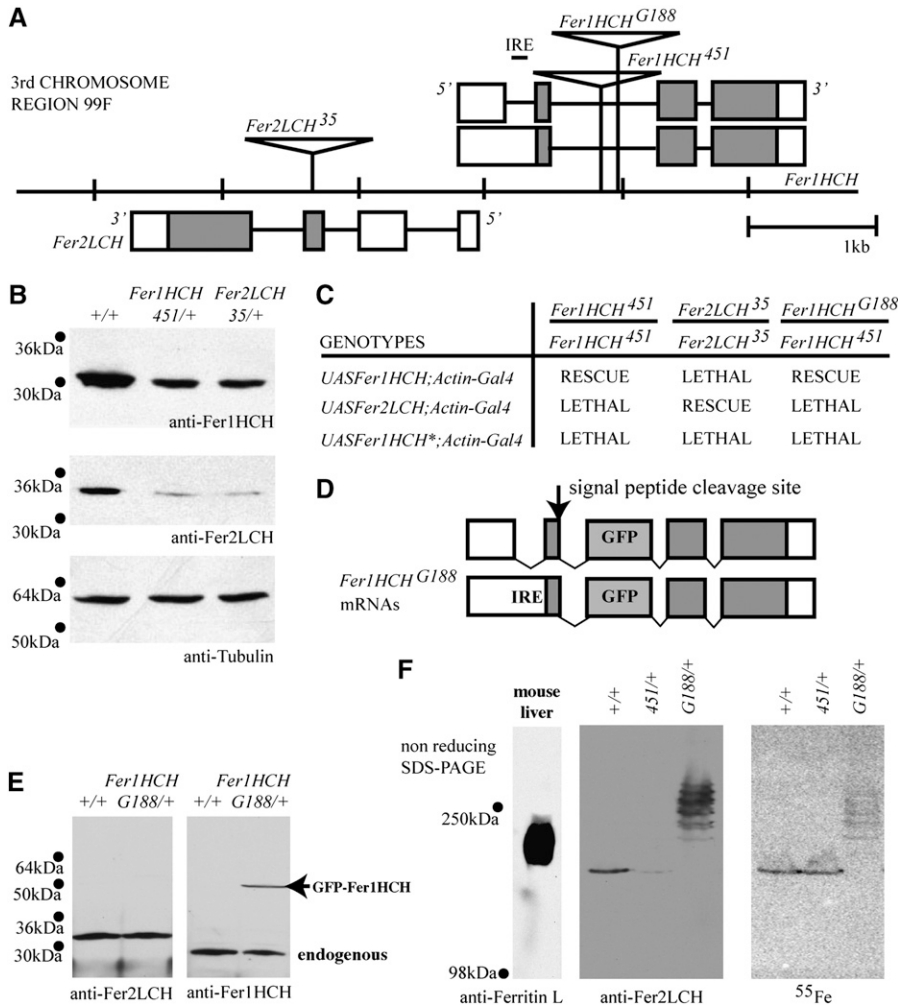


FIGURE 2.—Characterization of *Drosophila* strains containing transposable elements in *Fer1HCH/Fer2LCH*. (A) *Fer1HCH* and *Fer2LCH* share the same genetic locus at polytene position 99F on the third chromosome. Open and shaded boxes represent UTRs and the ORFs, respectively. The genomic insertions of *P* elements are shown as triangles and described in the text. (B) Western blot analysis of whole fly extracts from wild-type flies or the heterozygous *Fer1HCH*^{451/+} and *Fer2LCH*^{35/+} flies. Antibodies used are indicated at the bottom of the images. Levels of both ferritin subunits are reduced irrespective of which gene is affected by the transposon insertion. (C) Transgene-dependent rescue of the embryonic lethality associated with *Fer1HCH*^{451/451} and *Fer2LCH*^{35/35} and *Fer1HCH*^{G188/451} demonstrates the specific functions provided by the two genes. *UASFer1HCH** has no ferroxidase activity and cannot support ferritin function *in vivo*. (D) Predicted transcripts generated from the chromosome bearing the *Fer1HCH*^{G188} *P* element are depicted, indicating that both IRE- and non-IRE-containing transcripts (LIND *et al.* 1998; GEORGIEVA *et al.* 1999) will encode GFP-tagged versions of the Fer1HCH subunit. Note that the predicted cleavage site for generation of the mature polypeptide is contained in the second exon of the *Fer1HCH* gene, prior to the GFP insertion. (E) Protein extracts from wild-type and *Fer1HCH*^{G188/+} adult flies were subjected to reducing SDS-PAGE; Western

blots were probed with Fer2LCH and Fer1HCH peptide antibodies. Fer2LCH levels remain unchanged between the two samples, whereas there is less Fer1HCH and a higher-molecular-weight species appearing in *Fer1HCH*^{G188/+}, migrating at the predicted size for a GFP-Fer1HCH fusion protein. (F) Nonreducing SDS-PAGE separation of lysates from mouse liver and wild-type, *Fer1HCH*^{451/+}, and *Fer1HCH*^{G188/+} *Drosophila* strains. Flies were allowed to feed for 24 hr on food containing ⁵⁵FeCl₃-NTA. (Left) Western blots; (right) autoradiograph of a portion of the gel run in parallel. All detectable iron in extracts from *Fer1HCH*^{G188/+} flies coincides with the ferritin heteropolymers specific to this strain. Higher-molecular-weight species bands most probably reflect different ratios of native and GFP-tagged Fer1HCH subunits within ferritin heteropolymers.

was not able to functionally substitute for *Fer1HCH* and rescue the lethality of *Fer1HCH*^{451/451} flies. Thus, the ferroxidase activity of Fer1HCH provides an essential function *in vivo* and is likely required for iron loading of the ferritin shell.

Genetic and biochemical characterization of the GFP-ferritin trap line: A GFP-containing *P* element integrated into the second intron of *Fer1HCH* was used to study ferritin expression (Figure 2A) (MORIN *et al.* 2001). Intron/exon donor and acceptor splice sites flank the GFP sequence on the *P* element; consequently, all *Fer1HCH*^{G188} mRNA types (IRE +/-) are predicted to contain the GFP exon, which should encode GFP in frame with the Fer1HCH protein (Figure 2D). Therefore, post-transcriptional regulation of GFP-Fer1HCH mediated by the IRP-1A (LIND *et al.* 2006) would remain unaffected by the GFP exon. GFP is inserted two amino

acids downstream of the predicted cleavage site for the Fer1HCH signal peptide (CHARLESWORTH *et al.* 1997), which is encoded from the second exon of the gene (Figure 2D). Thus, the full-length mature polypeptide is predicted to translocate to the endoplasmic reticulum and contain the GFP attached to the N terminus, after the signal peptide is cleaved.

To test whether the GFP-Fer1HCH fusion polypeptide was generated as predicted from the locus containing the *G188* *P* element, extracts from adult wild-type (+/+) flies or flies heterozygous for the GFP-insertion line (*G188/+*) were separated by SDS-PAGE electrophoresis under reducing conditions. Western blots were probed with antisera raised against Fer1HCH or Fer2LCH peptides (Figure 2E). Results indicated the presence of two immunoreactive bands with the Fer1HCH antibody in *Fer1HCH*^{G188/+} lysates (Figure 2E, right blot). The

higher-molecular-weight species migrated at the predicted size of 50 kDa, consistent with a 27-kDa GFP addition to the 23-kDa Fer1HCH chain. Levels of the Fer2LCH did not change compared to wild-type lysates (Figure 2E, left blot).

To address whether the expressed GFP-Fer1HCH polypeptide contributed to the formation of the holoferritin in the transgenic insect, we separated the same extracts used in Figure 2E by SDS-PAGE electrophoresis under nonreducing conditions, which have previously been shown to preserve higher-molecular-weight ferritin heteropolymers (MISSIRLIS *et al.* 2006). In extracts from wild-type flies we observed a single ferritin species that migrated close to mouse liver ferritin (Figure 2F, left blots). As expected from the lower levels of both ferritin subunits in *Fer1HCH^{G188/451}* heterozygotes, these flies expressed less total ferritin. Conversely, in extracts from heterozygous *Fer1HCH^{G188/+}* flies that expressed GFP-tagged ferritin, several higher-molecular-weight bands could be detected. Thus, ferritin polymers are formed in these flies and the different molecular-weight species most likely reflect varying ratios of Fer1HCH and GFP-Fer1HCH chains in polymers. Importantly, no ferritin composed solely of native Fer1HCH and Fer2LCH was detected in the heterozygous *Fer1HCH^{G188/+}* flies, suggesting that the GFP-tagged ferritins are the functional ferritins of these animals. However, homozygous *Fer1HCH^{G188/G188}* and heteroallelic *Fer1HCH^{G188/451}* embryos failed to develop into larvae, indicating that the fly cannot survive when all Fer1HCH subunits are tagged with GFP. We wondered if GFP tagging of all Fer1HCH subunits hindered ferritin assembly or whether it obstructed access of an iron carrier to the assembled ferritin. If failure to assemble ferritin with 12 GFP-Fer1HCH subunits was the cause of lethality, we expected to rescue the lethality of *Fer1HCH^{G188/451}* flies by overexpression of the mutant ferroxidase construct *UAS-Fer1HCH**. This expectation arose from the fact that GFP-Fer1HCH should provide intact ferroxidase centers to the holomer, and mutant Fer1HCH* should allow normal assembly. However, overexpression of wild-type *UAS-Fer1HCH* rescued the lethality of *Fer1HCH^{G188/451}* flies, but *UAS-Fer1HCH** did not (Figure 2C), suggesting that a more likely explanation for the lethality of embryos expressing only GFP-Fer1HCH subunits is that the GFP tag blocks Fer1HCH-interacting proteins from accessing the ferroxidase centers of holoferritin.

GFP-ferritin is iron loaded: We sought to demonstrate that the GFP-tagged ferritin in the *Fer1HCH^{G188/+}* heterozygous flies was indeed able to sequester iron and substitute for nontagged holoferritin. To this end, we fed adult flies with radioactive iron in the form of $^{55}\text{FeCl}_3$. Nitrotriacetate was added to maintain $^{55}\text{Fe}^{3+}$ in solution at the neutral pH of food, and whole-fly homogenates were prepared after the insects were allowed to feed for 24 hr. Autoradiographs of the non-denaturing SDS-PAGE gels clearly indicated that iron

was incorporated in ferritin from wild-type or *Fer1HCH^{G188/+}* flies (Figure 2F, right, lanes 1 and 2) but also in GFP-tagged ferritin (Figure 2F, right, lane 3).

The observation that the same amount of iron was associated with half the amount of ferritin protein in the heterozygous *Fer1HCH^{G188/+}* strain (Figure 2F, middle lanes) suggests that the iron load per ferritin holomer can increase when total ferritin decreases. Also, the absence of ^{55}Fe incorporation in the heterozygous *Fer1HCH^{G188/+}* strain at the same molecular weight where putative residual normal ferritins would run suggests that these flies survive on ferritin containing both GFP-tagged and nontagged Fer1HCH subunits. Our speculation that GFP may partially inhibit iron loading is consistent with our findings that assembled ferritin molecules with fewer GFP tags (distinguished by their faster migration on Figure 2F) are more heavily iron loaded than assembled ferritin molecules with many GFP-Fer1HCH subunits (migrating more slowly on Figure 2F). Thus, although the GFP-Fer1HCH *in solo* is not fully functional, it coassembles *in vivo* with Fer1HCH to form functional fluorescent ferritin.

Overexpression of ferritin requires coexpression of both H and L subunits: Since iron overload is known to induce ferritin expression in vertebrates and flies alike, we sought to test the consequences of overexpression of either ferritin H or L genes under normal or low iron levels. Immunoblotting of lysates prepared from whole fly extracts revealed that ubiquitous overexpression of either of the two single chains individually was not sufficient to significantly alter total ferritin amounts or the relative ratio between the two chains (Figure 3A). In contrast, when both *UAS-Fer1HCH* and *UAS-Fer2LCH* were simultaneously activated with the same *Actin-Gal4* driver, robust overexpression was achieved in both sexes. Expression of the ferroxidase inactive *UAS-Fer1HCH** was also demonstrated when coexpressed with *UAS-Fer2LCH* (Figure 3A, right). Overexpression of ferritin was also revealed when the proteins were separated in non-reducing gels (Figure 3C, left). We confirmed successful expression from the transgenes by performing RT-PCR using primers that were specific to the transgenic mRNA (Figure 3B).

Phenotypes associated with ferritin overexpression: Ferritin overexpression in mammalian cells causes functional iron deficiency due to iron chelation (COZZI *et al.* 2000; WILKINSON *et al.* 2006). However, no significant alteration of total radioactive iron associated with overexpressed ferritin was detected after 24 hr of feeding (Figure 3C, right). If the feeding period was extended for 5 days, a slight increase was seen in sequestration of radiolabeled iron into the ferritin of overexpressors (data not shown), but overall (see also Figure 2F) the results show that, at least in *Drosophila*, ferritin protein levels are not the determining factor controlling iron storage into ferritin. Overexpression of ferroxidase-inactive *UAS-Fer1HCH** together with *UAS-Fer2LCH* in

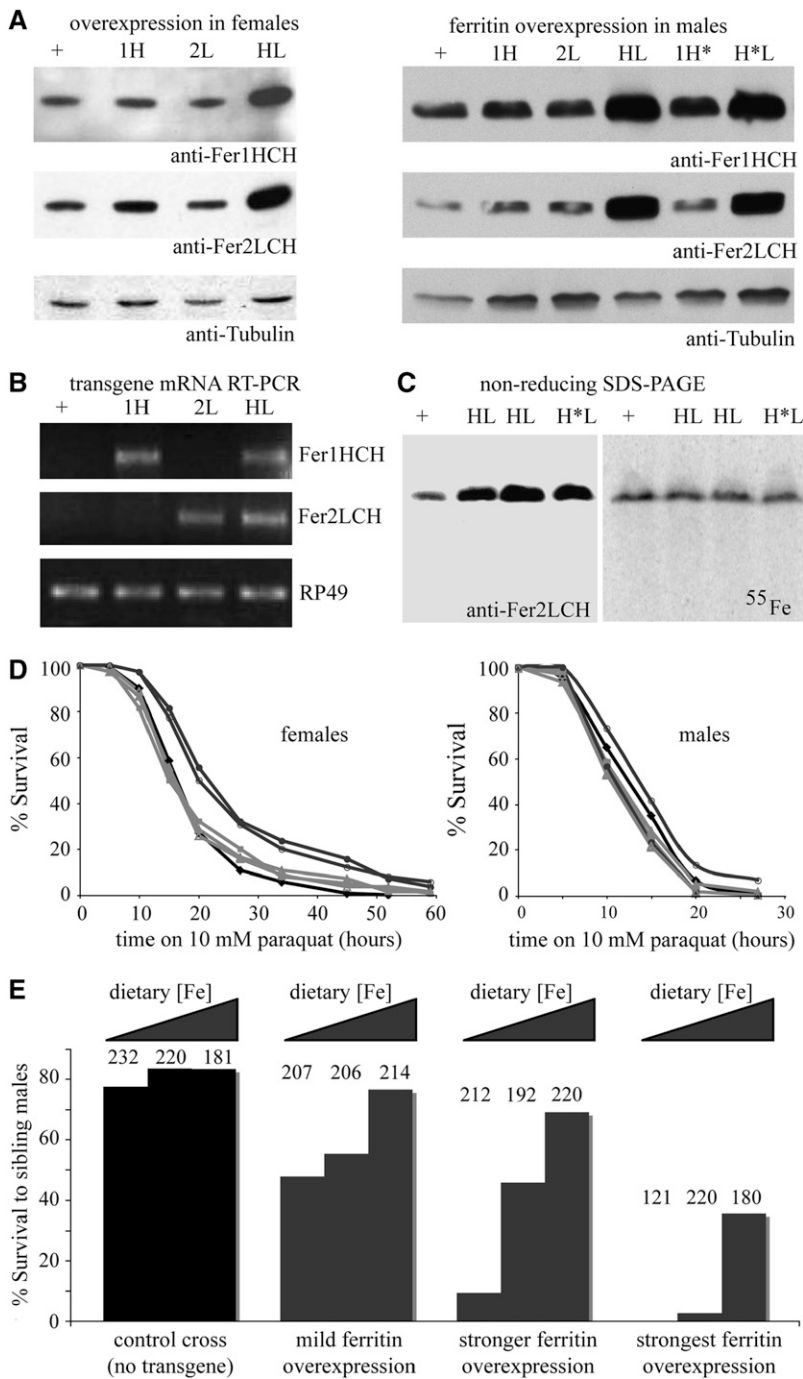


FIGURE 3.—Phenotypes associated with ubiquitous overexpression of ferritin. To achieve ferritin overexpression, we crossed homozygous female flies for the indicated transgene to males from the *Actin-Gal4/Cyo* stock. The progeny carrying the *Actin-Gal4* driver was selected. (A) Western blot analysis from whole fly extracts indicates that overexpression of the single-ferritin chains fails to alter their relative ratio. If a Fer1HCH or a Fer1HCH* subunit is overexpressed in parallel with Fer2LCH, significant overexpression is achieved. (B) To verify that transgenic message is expressed, RT-PCR was performed with primers specific to the UAS-derived transcripts. (C) Nonreducing SDS-PAGE separation of lysates from control, mild, and stronger ferritin overexpression strains, and the Fer1HCH*, Fer2LCH overexpression strain (genotypes are indicated in MATERIALS AND METHODS). Flies were allowed to feed for 24 hr on food containing ⁵⁵FeCl₃-NTA. (Left) Western blot probed with anti-Fer2LCH. (Right) An autoradiograph of a portion of the gel run in parallel. Interestingly, similar amounts of total iron are contained in the different size pools of total ferritin. Ferritin containing a mixture of functional endogenous Fer1HCH and nonfunctional transgene-derived Fer1HCH* subunits is still able to bind iron. (D) Survival on 10 mM paraquat is enhanced in female, but not male flies overexpressing ferritin. The solid line represents the control +/+; *Actin-Gal4*/+ flies, the three lightly shaded lines represent flies in which the single Fer1HCH, Fer2LCH, and Fer1HCH* are overexpressed (but not stabilized), while the two darkly shaded lines represent ferritin overexpressors (1H, 2L and 1H*, 2L). (E) Parental crosses were set up in vials containing 180 μM Bathophenanthroline disulfate to cause iron deficiency, regular food or 5 mM ferric ammonium citrate to cause iron overload. Male progeny of flies overexpressing ferritin (*i.e.*, carrying the *Actin-Gal4* driver) surviving to adulthood are compared to flies where ferritin overexpression is not induced from the transgene (*i.e.*, carrying the *Cyo* balancer chromosome). The number of flies counted containing the *Cyo* balancer chromosome is indicated at the top of each bar. Different levels of ferritin overexpression were achieved by using independent recombinant chromosomes and their combination. Iron deficiency combined with ferritin overexpression can be lethal, whereas ferritin overexpression is well tolerated under conditions of iron overload.

the presence of functional endogenous Fer1HCH subunits results in ferritin heteropolymers that are still potent iron-storage complexes.

We have recently shown that overexpression of Fer3HCH, a homopolymeric mitochondrial ferritin composed entirely of Fer3HCH chains, caused female-specific resistance to paraquat (MISSIRLIS *et al.* 2006). Here we show that overexpression of Fer1HCH or Fer2LCH alone is not sufficient to confer paraquat resistance, but coexpression of either Fer1HCH or Fer1HCH* in

concert with Fer2LCH confers greater survival to a paraquat challenge (Figure 3D), underscoring the functional cooperation of the ferritin subunits *in vivo*. As with flies overexpressing mitochondrial ferritin, resistance to oxidative stress is not observed in males that overexpress Fer1HCH and Fer2LCH (Figure 3D, right). These results were corroborated by using different driver lines (FB-Gal4 and Elav-Gal4) and also by using hydrogen peroxide as a stressor (data not shown). We speculate that overexpression of ferritin triggers a developmental

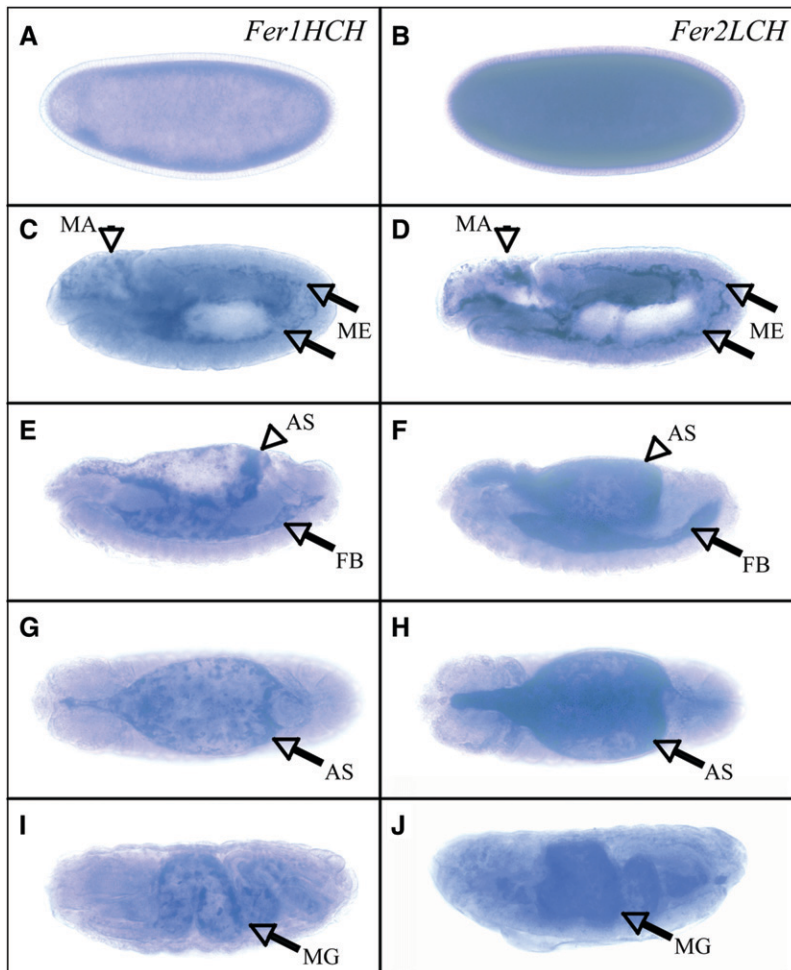


FIGURE 4.—Embryonic expression patterns of the two ferritin genes are similar. Detection of *Fer1HCH* and *Fer2LCH* transcripts by *in situ* hybridization of antisense RNAs to whole-mount preparations of embryos. Probe used for detection is indicated on top right of each column; the two genes are expressed in identical patterns. All images are oriented with anterior to the left. (A and B) High levels of staining in the blastoderm stage suggest that both transcripts are contributed from the mother to the embryo. (C and D) At germ-band elongation, transcripts accumulate in mesoderm (ME) and in the head region, where the macrophage lineage (MA) is specified. (E and F) During germ-band retraction, the fat bodies (FB) and amnioserosa (AS) are stained. (G and H) A dorsal view of the amnioserosa. (I and J) Midgut (MG) expression at late stages of embryogenesis.

signal, possibly related to iron availability, that is specific in females and could relate to the complex nutritional regulation that allocates resources toward reproduction, energy storage, or metabolic activity, all adaptive traits in females (BAUER *et al.* 2006).

In contrast to *Fer3HCH* overexpression, which did not affect development, flies overexpressing *Fer1HCH* and *Fer2LCH* are at a developmental disadvantage compared to their siblings (Figure 3E). We scored the progeny from the cross *Actin-Gal4/Cyo* × *UAS-Fer1HCH*, *UAS-Fer2LCH/UAS-Fer1HCH*, *UAS-Fer2LCH* by gender and by presence or absence of the *Actin-Gal4* driver. We used two independent sets of recombinant chromosomes (one on the X and one on the third) for *UAS-Fer1HCH* and *UAS-Fer2LCH* and also flies that carried both recombinant chromosomes, allowing for testing if the phenotype was dosage sensitive. We show the results in male flies (Figure 3E), where the competitive disadvantage of ferritin overexpression is more pronounced than in females. Importantly, the effects of ferritin overexpression are more dramatic under iron-limiting conditions induced by addition of the iron chelator Bathophenanthroline disulfate in the food, whereas the lethal effects can be rescued by dietary iron

supplementation. Therefore, our results indicate that ubiquitous ferritin overexpression in the absence of iron overload can be deleterious, by a mechanism that implicates the iron-chelating properties of ferritin.

Ferritin transcripts have similar expression patterns during embryogenesis: The genomic proximity between *Fer1HCH* and *Fer2LCH* could facilitate similar expression patterns to coordinate biosynthesis of the ferritin heteropolymer. *In situ* hybridizations of antisense RNA probes against the two genes in whole mount preparations of embryos at different stages of development were performed. We reasoned that if the predominant sites of *Fer1HCH* and *Fer2LCH* expression were different, it would be unlikely that they shared common regulatory enhancers, as previously suggested (DUNKOV and GEORGIEVA 1999, 2006). Nevertheless, we found that the different transcripts were expressed in highly specific, yet similar, patterns during embryogenesis (Figure 4). *Fer1HCH* and *Fer2LCH* were expressed during oogenesis and the maternal transcripts became evenly distributed in the egg and early embryo (data not shown), where they could be detected in the blastoderm (Figure 4, A and B). Tissue-specific transcripts were first detected during germ-band elongation in cells of the

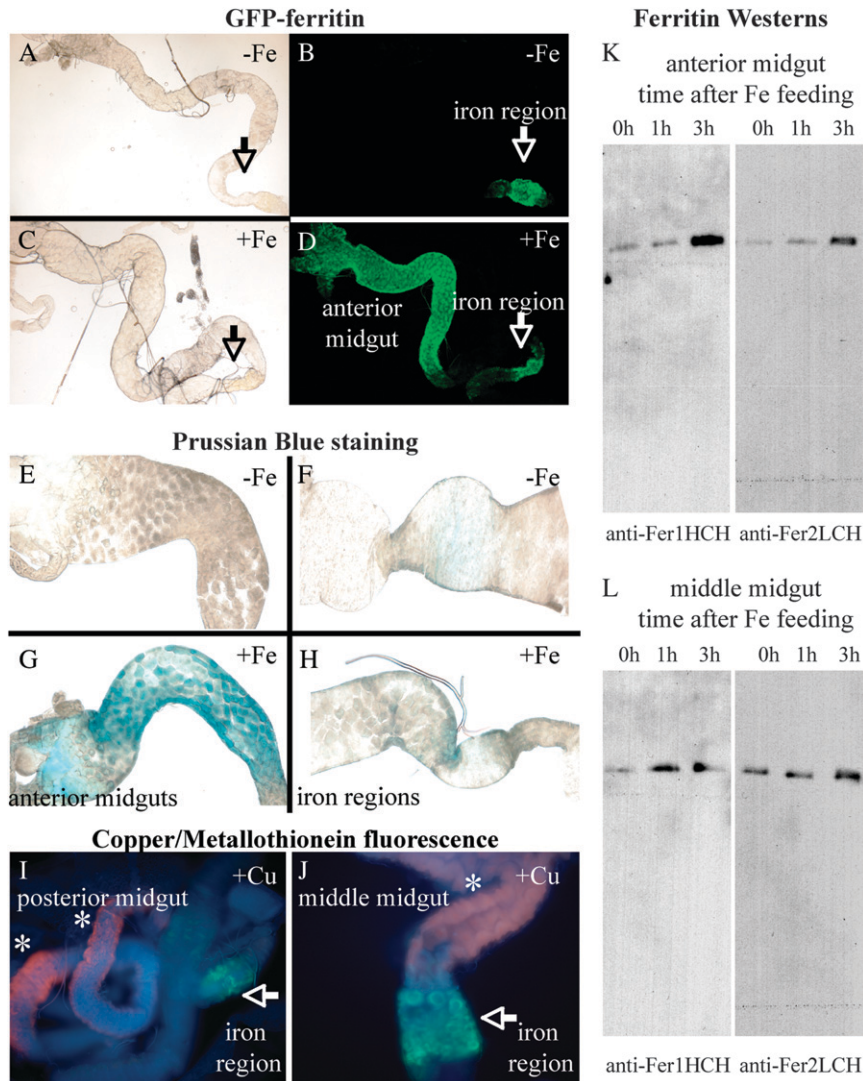


FIGURE 5.—Intestinal sites of constitutive and inducible ferritin expression differ. (A and B) Dissected larval midgut from the *Fer1HCH^{G188/+}* line. Fluorescence identifies the iron region in the middle midgut (arrows). (C and D) Dissected midgut from larvae of the same genotype raised on food containing 1 mM ferric ammonium citrate. Note that ferritin protein accumulates in the anterior midgut. (E–H) Prussian blue staining of midguts from control or iron-fed larvae: (E) anterior midgut, control diet; (F) iron region, control diet; (G) anterior midgut, iron diet; (H) iron region, iron diet. (I and J) *Fer1HCH^{G188/+}* larvae were raised on food containing 1 mM CuSO_4 and midguts were imaged using UV excitation and the DAPI filter. (I) Cu-metallothionein fluorescence (orange, asterisks) is prominent in the posterior midgut. (J) Cu-metallothionein fluorescence is also found in a cluster of cells anterior to the iron region, where constitutive metallothionein expression has been reported (MCNULTY *et al.* 2001). (K and L) Time course of iron-dependent ferritin induction in (K) anterior midgut and (L) middle midgut dissected from third instar larvae. Extracts were subjected to electrophoresis under nonreducing conditions and analyzed by immunoblotting. Ferritin induction in the iron region is much less pronounced.

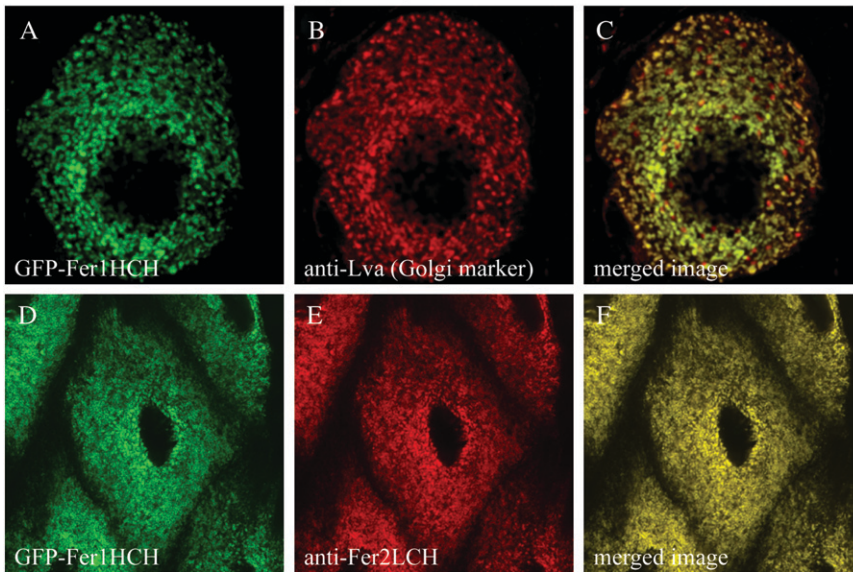
mesoderm (Figure 4, C and D), which are specified to give rise to the fat bodies and amnioserosa (Figure 4, E and F). Staining was also seen in cells destined to become macrophages in the anterior head region of embryos (Figure 4, C and D). During germ-band retraction and dorsal closure, the amnioserosa retained ferritin mRNAs (Figures 4, G and H). At late stages of embryogenesis, cells in the developing midgut initiated ferritin transcription (Figure 4, I and J). The similar embryonic expression patterns of *Fer1HCH* and *Fer2LCH* suggest that both ferritin subunits are expressed in each cell type where ferritin is required.

Ferritin expression and iron homeostasis in the larval midgut: Ferritin is abundant in the midguts from several different insect species and its expression is induced by dietary iron (CAPURRO MDE *et al.* 1996; DUNKOV *et al.* 2002; GEORGIEVA *et al.* 2002; KIM *et al.* 2002). We showed earlier that GFP-tagged ferritin stores iron in *Fer1HCH^{G188/+}* flies. We next wanted to determine if the expression pattern of GFP-tagged ferritin was similar to that of the endogenous nontagged protein.

Indeed, GFP-tagged ferritin was most prominently expressed in a cluster of cells of the middle midgut (Figure 5, A and B). These cells have been identified as the iron region of the insect midgut on the basis of their positive stain with Prussian blue and the accumulation of exogenously administered radioactive iron (POULSON and BOWEN 1952). Mid-third instar larvae were administered a diet containing 5 mM ferric ammonium citrate and their intestines were dissected for imaging. GFP-tagged ferritin was inducible only in cells of the anterior midgut, but was constitutively expressed in the iron region of the middle midgut and no expression was detected in the copper cells that are present in between the two regions (Figure 5, A–D).

Midguts from larvae subjected to the same treatment were also stained with Prussian blue (Figure 5, E–H). A light blue staining indicative of the presence of ferric iron was observed in the iron region of both iron-fed and control larvae and was largely unchanged by feeding on an iron-enriched diet (Figure 5, F and H). In contrast, the anterior region was not stained in control larvae

Imaging of single cell in iron region



Time-course after Fe feeding; imaging of single cell in anterior midgut

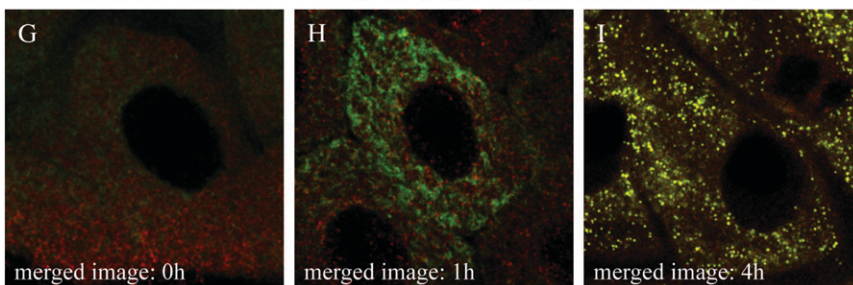


FIGURE 6.—Ferritin resides in the Golgi apparatus of midgut cells. (A) Section of a single cell in the iron region of a dissected midgut from *Fer1HCH^{G188/+}* larvae imaged by confocal microscopy. Note the punctate subcellular localization, consistent with membrane-enclosed ferritin compartments seen by EM in midgut preparations from another insect species (LOCKE and LEUNG 1984). (B) The same cell was stained with anti-Lava lamp, a Golgi-associated protein. (C) Yellow identifies the Golgi complex as the primary location of ferritin in cells of the iron region. (D–F) A single cell expressing GFP-Fer1HCH in the iron region was stained with anti-Fer2LCH; colocalization of the ferritin chains was seen in the Golgi. (G–I) Time course of ferritin induction in single cells of the anterior midgut. Merged images of GFP-Fer1HCH in green and Fer2LCH in red are shown. (G) Prior to iron feeding, low levels of the ferritin subunits are expressed. (H) One hour post-feeding, GFP-Fer1HCH is in the endoplasmic reticulum, while Fer2LCH is detected only in Golgi bodies. (I) Four hours post-feeding, the two chains colocalize in the Golgi apparatus.

(Figure 5E), but stained dark blue in iron-fed individuals (Figure 5G), indicating that the ferritin that accumulates in the anterior midgut upon iron feeding is rich in iron content.

To assess the time frame of ferritin induction during iron feeding and to further demonstrate that a specific subset of cells in the anterior midgut shows a strong response to iron levels, we determined endogenous ferritin levels in a time course following iron feeding. For this experiment we used wild-type third instar larvae (100 hr old at 25°) and dissected their anterior and middle midguts for Western blot analysis. The results showed a clear induction of the ferritin heteropolymers 3 hr postfeeding in the anterior midgut (Figure 5K). Consistent with our imaging and iron-staining results, the induction of ferritin was largely restricted to the anterior midgut and was much less pronounced in the iron region (Figure 5L).

Another essential transition metal and dietary nutrient for *Drosophila* is copper (ZHOU *et al.* 2003; SELVARAJ *et al.* 2005). Copper-containing (cuprophilic) cells function in the acidification of the midgut and are present at different sites than the iron region (POULSON and BOWEN 1952; HOPPLER and BIENZ 1994; DUBREUIL *et al.* 2001). Copper-metallothionein complexes in these cells

fluoresce orange–red upon ultraviolet illumination (MCNULTY *et al.* 2001). We imaged simultaneously the copper-metallothionein fluorescence and GFP-ferritin in midguts from larvae fed a diet containing 1 mM Cu²⁺. The results showed that ferritin-expressing cells indeed form a distinct cellular population from cells that contain copper (Figure 5, I and J; see also DISCUSSION).

Ferritin induction at subcellular resolution: To investigate which cellular compartment accumulates iron-loaded ferritin in midgut cells, we costained GFP-Fer1HCH-expressing cells with an antibody raised against the Golgi-associated protein Lava lamp (SISSEON *et al.* 2000). Confocal images from a single cell in the iron region clearly showed that all GFP-ferritin localized within the Golgi compartment (Figure 6, A–C), consistent with the images obtained by electron microscopy (LOCKE and LEUNG 1984; NICHOL and LAW 1990). A few Golgi bodies in cells from the iron region were devoid of ferritin (Figure 6C, red). We also imaged the same cells stained with antibodies against the Fer2LCH subunits. As expected from their tight association revealed by structural studies, biochemical analysis, and electron microscopy, there was complete colocalization with GFP-Fer1HCH in the Golgi complex of these specialized cells (Figure 6, D–F). Finally, we focused on the cells of the

anterior midgut that do not normally express ferritin, but potentially do so in the presence of high iron levels (see Figure 5, A–D). The cells were stained for both ferritin chains during the time course of ferritin induction (Figure 6, G–I). Prior to iron feeding, GFP-Fer1HCH was not expressed and low levels of Fer2LCH were detected (Figure 6G). At 1 hr postinduction GFP-Fer1HCH was detected in a compartment resembling the endoplasmic reticulum, but we could also detect Fer2LCH-positive Golgi that were devoid of GFP-Fer1HCH subunits (Figure 6H). In contrast, at 4 hr postinduction the two subunits were strongly induced and were seen only in complex with one another within the Golgi (Figure 6I).

Collectively, our results have identified different specialized intestinal sites for iron and copper metabolism and showed that ferritin synthesis is differentially regulated along the intestine. Significantly, our results also validate the use of the *Fer1HCH*^{G188} line as a faithful reporter of endogenous ferritin expression.

DISCUSSION

Several novel findings on *Drosophila* ferritin are described in this work. We show that the absence of either Fer1HCH or Fer2LCH results in embryonic lethality and that modified Fer1HCH subunits (mutant in the ferroxidase center or GFP tagged) cannot substitute for lack of Fer1HCH. However, if the same modified subunits are expressed in the presence of wild-type subunits, they can be integrated into ferritin holomers without inducing dominant-negative effects. Analysis of heterozygous loss-of-function ferritin fly mutants or flies overexpressing ferritin subunits revealed that a constant ratio of Fer1HCH and Fer2LCH is maintained, independent of their internal transcriptional expression levels. The structural cooperation of the two subunits that is secured via disulfide bonds (HAMBURGER *et al.* 2005) likely explains these observations. A post-transcriptional mechanism, possibly involving the degradation of subunits that are present in excess, ensures the presence of equal amounts of the two subunits. Such a mechanism can explain the absence of the IRE in *Fer2LCH* mRNAs in insects, since Fer1HCH translational repression by IRP-1A under iron-limiting conditions (that favor the IRE-containing transcripts; GEORGIEVA *et al.* 1999) would then be sufficient to reduce levels of Fer2LCH.

In contrast to results from mammalian cell or animal models (THOMPSON *et al.* 2003; WILKINSON *et al.* 2006), but consistent with what is known from human patients with hereditary hyperferritinemia cataract syndrome (CAZZOLA 2002), experimental reduction or increase of ferritin levels through genetic manipulation in *Drosophila* caused only very mild alterations in the insect's iron homeostasis. These results point toward an independent regulatory system that controls iron se-

questration into ferritin. The nature of this system is currently unknown, but could involve a putative iron chaperone that delivers iron to ferritin (NAPIER *et al.* 2005). However, the hypothesized chaperone's function does not completely override the need for ferritin regulation, as shown by the phenotype of ferritin overexpressing flies that was lethal under low iron conditions, but was rescued with iron supplementation (Figure 3E). Alternatively, localization of ferritin in the Golgi apparatus of insect cells may prevent it from contact with the cytosolic and mitochondrial iron pools. It is currently not known how iron is delivered to the ferritin that resides in the secretory pathway of cells.

We provided evidence that the ferritin genes are co-expressed during embryogenesis. We wondered whether their genetic proximity is conserved in other *Drosophila* species with fully sequenced genomes. To this end, we used the EvoPrinter, a new multigenomic DNA sequence analysis tool that facilitates the rapid identification of evolutionarily conserved sequences within the context of a single species (ODENWALD *et al.* 2005). *In silico* analysis of the *Fer1HCH* and *Fer2LCH* genomic locus by the EvoPrinter produced an output of the combined mutational histories of six *Drosophila* species, superimposed on a reference sequence from *D. melanogaster* (supplemental Figure 1 at <http://www.genetics.supplemental/>). The results not only showed that clustering of the two genes is conserved, but also identified potentially shared regulatory regions. From the 17,670 bp spanning the two genes that were analyzed, only 914 (or 5.2%) were conserved in an identical position in all six species tested. One-third of these conserved sequences (306) were contained within the open reading frames. Surprisingly, over half of them (491) were not contained in the cDNA sequence, but rather were clustered in two regions: downstream of the *Fer2LCH*-transcribed region or in the second intron of *Fer1HCH* (supplemental Figure 1). A particular stretch of 10 bp, TTTGCACACG, was found three times in the second intron of *Fer1HCH* and could represent a binding site for an unidentified factor. The remaining conserved base pairs (117) were mostly concentrated in the 5'-UTR of *Fer1HCH*, including the IRE itself. The conservation of the IRE over ~160 million years of collective evolutionary divergence underscores the functional significance of the IRE/IRP control system in all *Drosophila* species.

Ferritin regulation is a critical aspect of the organism's iron economy. Our finding that ferritin expression in the iron region is constitutive (and remains so even under iron-deficient conditions), but is inducible in the anterior midgut, has a parallel with the expression of metallothioneins, which are the copper storage proteins (EGLI *et al.* 2006). Interestingly, cuprophilic cells that are present anterior to the iron region show constitutive metallothionein expression (MCNULTY *et al.* 2001), whereas cells in both the anterior and posterior midgut induce

metallothionein expression and copper/metallothionein fluorescence at higher copper concentrations (POULSON and BOWEN 1952; MCNULTY *et al.* 2001) (Figure 5J). Results presented in this article, combined with previous reports, lead to the following fundamental conclusion with respect to metal metabolism in the midgut of *Drosophila*: the insect midgut contains two sets of specialized cells, one of which constitutively expresses metallothionein and a second constitutively expresses ferritin. If either metal is present in great abundance, a third and fourth set of distinct midgut cells have the potential to induce transcription of the genes that encode the two metal storage proteins. Importantly, there are also cells in the midgut that do not respond significantly to high concentrations of these metals. Whether similar cellular populations exist in the mammalian intestine remains unknown, but cellular populations with specific metal contents were recently described in plant seeds (KIM *et al.* 2006).

The GFP-tagged ferritin that we have described in *Drosophila* revealed the complex physiologic orchestration of intestinal metal responses. In addition, it has enabled visualization of subcellular ferritin dynamics upon iron-mediated induction and should facilitate the dissection and subcellular localization of ferritin biosynthesis and trafficking. Serum ferritin is measured in clinical practice as a measure of total-body iron stores (BEUTLER *et al.* 2002) and is an acute phase reactant (TRAN *et al.* 1997) but few studies have addressed how ferritin is secreted in the circulatory system of humans (GHOSH *et al.* 2004; RENAUD *et al.* 1991). Importantly, ferritin tagged with GFP could function and elucidate trafficking mechanisms in human cells (DE DOMENICO *et al.* 2006) and transgenic mice (COHEN *et al.* 2007).

The authors thank Foteini Mourkioti and Herbert Jäckle for help with the generation of the *UAS-Fer1HCH* and *UAS-Fer2LCH* transgenic flies and Genetic Services for the *UAS-Fer1HCH** transgenic flies. We especially thank Mary Lilly for offering lab space and fly-pushing support to members of the Cell Biology and Metabolism Branch of the National Institute of Child Health and Human Development (NICHD). We thank Wing-Hang Tong and Kuanyu Li for intellectual inputs. The intramural programs of the NICHD and the National Institute of Neurological Disorders and Stroke supported this work.

Note added in proof: The conserved stretch of 10 bp, TTTGCACACG, identified here by EvoPrinter analysis of the *Fer1HCH* and *Fer2LCH* genomic locus has been independently described by others (H. YEPISKOPOSYAN, D. EGLI, T. FERGESTAD, A. SELVARAJ, C. TREIBER *et al.*, 2006, Transcriptome response to heavy metal stress in *Drosophila* reveals a new zinc transporter that confers resistance to zinc. *Nucleic Acids Res.* **34**: 4866–4977). These authors have previously characterized the binding of metal transcription factor 1 to this sequence.

LITERATURE CITED

- BAUER, M., J. D. KATZENBERGER, A. C. HAMM, M. BONAUS, I. ZINKE *et al.*, 2006 Purine and folate metabolism as a potential target of sex-specific nutrient allocation in *Drosophila* and its implication for lifespan-reproduction tradeoff. *Physiol. Genomics* **25**: 393–404.
- BEUTLER, E., V. FELITTI, N. J. HO and T. GELBART, 2002 Relationship of body iron stores to levels of serum ferritin, serum iron, unsaturated iron binding capacity and transferrin saturation in patients with iron storage disease. *Acta Haematol.* **107**: 145–149.
- BRAND, A. H., and N. PERRIMON, 1993 Targeted gene expression as a means of altering cell fates and generating dominant phenotypes. *Development* **118**: 401–415.
- BRODY, T., C. STIVERS, J. NAGLE and W. F. ODENWALD, 2002 Identification of novel *Drosophila* neural precursor genes using a differential embryonic head cDNA screen. *Mech. Dev.* **113**: 41–59.
- CAPURRO MDE, L., P. IUGHETTI, P. E. RIBOLLA and A. G. DE BIANCHI, 1996 *Musca domestica* hemolymph ferritin. *Arch. Insect Biochem. Physiol.* **32**: 197–207.
- CAZZOLA, M., 2002 Hereditary hyperferritinaemia/cataract syndrome. *Best Pract. Res. Clin. Haematol.* **15**: 385–398.
- CHARLESWORTH, A., T. GEORGIEVA, I. GOSPODOV, J. H. LAW, B. C. DUNKOV *et al.*, 1997 Isolation and properties of *Drosophila melanogaster* ferritin—molecular cloning of a cDNA that encodes one subunit, and localization of the gene on the third chromosome. *Eur. J. Biochem.* **247**: 470–475.
- COHEN, B., K. ZIV, V. PLAKS, T. ISRAELY, V. KALCHENKO *et al.*, 2007 MRI detection of transcriptional regulation of gene expression in transgenic mice. *Nat. Med.* **13**: 498–503.
- COOPERMAN, S. S., E. G. MEYRON-HOLTZ, H. OLIVIERRE-WILSON, M. C. GHOSH, J. P. MCCONNELL *et al.*, 2005 Microcytic anemia, erythropoietic protoporphyria, and neurodegeneration in mice with targeted deletion of iron-regulatory protein 2. *Blood* **106**: 1084–1091.
- COZZI, A., B. CORSI, S. LEVI, P. SANTAMBROGIO, A. ALBERTINI *et al.*, 2000 Overexpression of wild type and mutated human ferritin H-chain in HeLa cells: in vivo role of ferritin ferroxidase activity. *J. Biol. Chem.* **275**: 25122–25129.
- DE DOMENICO, I., M. B. VAUGHN, L. LI, D. BAGLEY, G. MUSCI *et al.*, 2006 Ferroportin-mediated mobilization of ferritin iron precedes ferritin degradation by the proteasome. *EMBO J.* **25**: 5396–5404.
- DUBREUIL, R. R., T. GRUSHKO and O. BAUMANN, 2001 Differential effects of a labial mutation on the development, structure, and function of stomach acid-secreting cells in *Drosophila melanogaster* larvae and adults. *Cell Tissue Res.* **306**: 167–178.
- DUNKOV, B., and T. GEORGIEVA, 2006 Insect iron binding proteins: insights from the genomes. *Insect Biochem. Mol. Biol.* **36**: 300–309.
- DUNKOV, B. C., and T. GEORGIEVA, 1999 Organization of the ferritin genes in *Drosophila melanogaster*. *DNA Cell Biol.* **18**: 937–944.
- DUNKOV, B. C., T. GEORGIEVA, T. YOSHIGA, M. HALL and J. H. LAW, 2002 *Aedes aegypti* ferritin heavy chain homologue: feeding of iron or blood influences message levels, lengths and subunit abundance. *J. Insect Sci.* **2**: 7.
- EGLI, D., H. YEPISKOPOSYAN, A. SELVARAJ, K. BALAMURUGAN, R. RAJARAM *et al.*, 2006 A family knockout of all four *Drosophila* metallothioneins reveals a central role in copper homeostasis and detoxification. *Mol. Cell Biol.* **26**: 2286–2296.
- GALY, B., D. FERRING, B. MINANA, O. BELL, H. G. JANSER *et al.*, 2005 Altered body iron distribution and microcytosis in mice deficient in iron regulatory protein 2 (IRP2). *Blood* **106**: 2580–2589.
- GALY, B., S. M. HOLTER, T. KLOPSTOCK, D. FERRING, L. BECKER *et al.*, 2006 Iron homeostasis in the brain: complete iron regulatory protein 2 deficiency without symptomatic neurodegeneration in the mouse. *Nat. Genet.* **38**: 967–969 discussion 969–970.
- GEORGIEVA, T., B. C. DUNKOV, N. HARIZANOVA, K. RALCHEV and J. H. LAW, 1999 Iron availability dramatically alters the distribution of ferritin subunit messages in *Drosophila melanogaster*. *Proc. Natl. Acad. Sci. USA* **96**: 2716–2721.
- GEORGIEVA, T., B. C. DUNKOV, S. DIMOV, K. RALCHEV and J. H. LAW, 2002 *Drosophila melanogaster* ferritin: cDNA encoding a light chain homologue, temporal and tissue specific expression of both subunit types. *Insect Biochem. Mol. Biol.* **32**: 295–302.
- GHOSH, S., S. HEVI and S. L. CHUCK, 2004 Regulated secretion of glycosylated human ferritin from hepatocytes. *Blood* **103**: 2369–2376.
- HAMBURGER, A. E., A. P. WEST, JR., Z. A. HAMBURGER, P. HAMBURGER and P. J. BJORKMAN, 2005 Crystal structure of a secreted insect ferritin reveals a symmetrical arrangement of heavy and light chains. *J. Mol. Biol.* **349**: 558–569.
- HARRISON, P. M., and P. AROSIO, 1996 The ferritins: molecular properties, iron storage function and cellular regulation. *Biochim. Biophys. Acta* **1275**: 161–203.
- HENTZE, M. W., M. U. MUCKENTHALER and N. C. ANDREWS, 2004 Balancing acts: molecular control of mammalian iron metabolism. *Cell* **117**: 285–297.

- HOPPLER, S., and M. BIENZ, 1994 Specification of a single cell type by a *Drosophila* homeotic gene. *Cell* **76**: 689–702.
- KAUR, D., F. YANTIRI, S. RAJAGOPALAN, J. KUMAR, J. Q. MO *et al.*, 2003 Genetic or pharmacological iron chelation prevents MPTP-induced neurotoxicity in vivo: a novel therapy for Parkinson's disease. *Neuron* **37**: 899–909.
- KAUR, D., S. RAJAGOPALAN, S. CHINTA, J. KUMAR, D. DI MONTE *et al.*, 2006 Chronic ferritin expression within murine dopaminergic midbrain neurons results in a progressive age-related neurodegeneration. *Brain Res.* **1140**: 188–194.
- KELSO, R. J., M. BUSZCZAK, A. T. QUINONES, C. CASTIBLANCO, S. MAZZALUPO *et al.*, 2004 Flytrap, a database documenting a GFP protein-trap insertion screen in *Drosophila melanogaster*. *Nucleic Acids Res.* **32**: D418–D420.
- KIM, B. S., C. S. LEE, J. Y. SEOL, C. Y. YUN and H. R. KIM, 2002 Cloning and expression of 32 kDa ferritin from *Galleria mellonella*. *Arch. Insect Biochem. Physiol.* **51**: 80–90.
- KIM, S. A., T. PUNSHON, A. LANZIROTTI, L. LI, J. M. ALONSO *et al.*, 2006 Localization of iron in *Arabidopsis* seed requires the vacuolar membrane transporter VIT1. *Science* **314**: 1295–1298.
- LAVAUTE, T., S. SMITH, S. COOPERMAN, K. IWAI, W. LAND *et al.*, 2001 Targeted deletion of the gene encoding iron regulatory protein-2 causes misregulation of iron metabolism and neurodegenerative disease in mice. *Nat. Genet.* **27**: 209–214.
- LEVI, S., A. COZZI and P. AROSIO, 2005 Neuroferritinopathy: a neurodegenerative disorder associated with L-ferritin mutation. *Best Pract. Res. Clin. Haematol.* **18**: 265–276.
- LIND, M. I., S. EKENGREN, O. MELEFORS and K. SODERHALL, 1998 *Drosophila* ferritin mRNA: alternative RNA splicing regulates the presence of the iron-responsive element. *FEBS Lett.* **436**: 476–482.
- LIND, M. I., F. MISSIRLIS, O. MELEFORS, H. UHRIGSHARDT, K. KIRBY *et al.*, 2006 Of two cytosolic aconitases expressed in *Drosophila*, only one functions as an iron-regulatory protein. *J. Biol. Chem.* **281**: 18707–18714.
- LOCKE, M., and H. LEUNG, 1984 The induction and distribution of an insect ferritin—a new function for the endoplasmic reticulum. *Tissue Cell* **16**: 739–766.
- M McNULTY, M., M. PULJUNG, G. JEFFORD and R. R. DUBREUIL, 2001 Evidence that a copper-metallothionein complex is responsible for fluorescence in acid-secreting cells of the *Drosophila* stomach. *Cell Tissue Res.* **304**: 383–389.
- MISSIRLIS, F., J. HU, K. KIRBY, A. J. HILLIKER, T. A. ROUAULT *et al.*, 2003 Compartment-specific protection of iron-sulfur proteins by superoxide dismutase. *J. Biol. Chem.* **278**: 47365–47369.
- MISSIRLIS, F., S. HOLMBERG, T. GEORGIEVA, B. C. DUNKOV, T. A. ROUAULT *et al.*, 2006 Characterization of mitochondrial ferritin in *Drosophila*. *Proc. Natl. Acad. Sci. USA* **103**: 5893–5898.
- MORIN, X., R. DANEMAN, M. ZAVORTINK and W. CHIA, 2001 A protein trap strategy to detect GFP-tagged proteins expressed from their endogenous loci in *Drosophila*. *Proc. Natl. Acad. Sci. USA* **98**: 15050–15055.
- MUCKENTHALER, M., N. GUNKEL, D. FRISHMAN, A. CYRKLAF, P. TOMANCAK *et al.*, 1998 Iron-regulatory protein-1 (IRP-1) is highly conserved in two invertebrate species—characterization of IRP-1 homologues in *Drosophila melanogaster* and *Caenorhabditis elegans*. *Eur. J. Biochem.* **254**: 230–237.
- NAPIER, I., P. PONKA and D. R. RICHARDSON, 2005 Iron trafficking in the mitochondrion: novel pathways revealed by disease. *Blood* **105**: 1867–1874.
- NICHOL, H., and J. H. LAW, 1990 The localization of ferritin in insects. *Tissue Cell* **22**: 767–777.
- NICHOL, H., J. H. LAW and J. J. WINZERLING, 2002 Iron metabolism in insects. *Annu. Rev. Entomol.* **47**: 535–559.
- ODENWALD, W. F., W. RASBAND, A. KUZIN and T. BRODY, 2005 EVOPRINTER, a multigenomic comparative tool for rapid identification of functionally important DNA. *Proc. Natl. Acad. Sci. USA* **102**: 14700–14705.
- PANTOPOULOS, K., 2004 Iron metabolism and the IRE/IRP regulatory system: an update. *Ann. NY Acad. Sci.* **1012**: 1–13.
- PHAM, C. G., C. BUBICI, F. ZAZZERONI, S. PAPA, J. JONES *et al.*, 2004 Ferritin heavy chain upregulation by NF-kappaB inhibits TNFalpha-induced apoptosis by suppressing reactive oxygen species. *Cell* **119**: 529–542.
- PONKA, P., 1997 Tissue-specific regulation of iron metabolism and heme synthesis: distinct control mechanisms in erythroid cells. *Blood* **89**: 1–25.
- POULSON, D. F., and V. T. BOWEN, 1952 Organization and function of the inorganic constituents of nuclei. *Exp. Cell Res. Suppl.* **2**: 161–180.
- RENAUD, D. L., H. NICHOL and M. LOCKE, 1991 The visualization of apoferritin in the secretory pathway of vertebrate liver cells. *J. Submicrosc. Cytol. Pathol.* **23**: 501–507.
- ROTHENBERGER, S., E. W. MULLNER and L. C. KUHN, 1990 The mRNA-binding protein which controls ferritin and transferrin receptor expression is conserved during evolution. *Nucleic Acids Res.* **18**: 1175–1179.
- ROUAULT, T. A., 2006 The role of iron regulatory proteins in mammalian iron homeostasis and disease. *Nat. Chem. Biol.* **2**: 406–414.
- ROUAULT, T. A., and W. H. TONG, 2005 Iron-sulphur cluster biogenesis and mitochondrial iron homeostasis. *Nat. Rev. Mol. Cell Biol.* **6**: 345–351.
- RUBIN, G. M., and A. C. SPRADLING, 1982 Genetic transformation of *Drosophila* with transposable element vectors. *Science* **218**: 348–353.
- SANTAMBROGIO, P., S. LEVI, A. COZZI, B. CORSI and P. AROSIO, 1996 Evidence that the specificity of iron incorporation into homopolymers of human ferritin L- and H-chains is conferred by the nucleation and ferroxidase centres. *Biochem. J.* **314**(Pt 1): 139–144.
- SELVARAJ, A., K. BALAMURUGAN, H. YEPISKOPOSYAN, H. ZHOU, D. EGLI *et al.*, 2005 Metal-responsive transcription factor (MTF-1) handles both extremes, copper load and copper starvation, by activating different genes. *Genes Dev.* **19**: 891–896.
- SISSON, J. C., C. FIELD, R. VENTURA, A. ROYOU and W. SULLIVAN, 2000 Lava lamp, a novel peripheral golgi protein, is required for *Drosophila melanogaster* cellularization. *J. Cell Biol.* **151**: 905–918.
- SMITH, S. R., S. COOPERMAN, T. LAVAUTE, N. TRESSER, M. GHOSH *et al.*, 2004 Severity of neurodegeneration correlates with compromise of iron metabolism in mice with iron regulatory protein deficiencies. *Ann. NY Acad. Sci.* **1012**: 65–83.
- SPRADLING, A. C., D. STERN, A. BEATON, E. J. RHEM, T. LAVERTY *et al.*, 1999 The Berkeley *Drosophila* Genome Project Gene Disruption Project: single P-element insertions mutating 25% of vital *Drosophila* genes. *Genetics* **153**: 135–177.
- THOMPSON, K., S. MENZIES, M. MUCKENTHALER, F. M. TORTI, T. WOOD *et al.*, 2003 Mouse brains deficient in H-ferritin have normal iron concentration but a protein profile of iron deficiency and increased evidence of oxidative stress. *J. Neurosci. Res.* **71**: 46–63.
- TORTI, F. M., and S. V. TORTI, 2002 Regulation of ferritin genes and protein. *Blood* **99**: 3505–3516.
- TRAN, T. N., S. K. EUBANKS, K. J. SCHAFFER, C. Y. ZHOU and M. C. LINDER, 1997 Secretion of ferritin by rat hepatoma cells and its regulation by inflammatory cytokines and iron. *Blood* **90**: 4979–4986.
- WILKINSON, J., X. DI, K. SCHÖNIG, J. L. BUSS, N. D. KOCK *et al.*, 2006 Tissue-specific expression of ferritin H regulates cellular iron homeostasis in vivo. *Biochem. J.* **395**: 501–507.
- ZHOU, H., K. M. CADIGAN and D. J. THIELE, 2003 A copper-regulated transporter required for copper acquisition, pigmentation, and specific stages of development in *Drosophila melanogaster*. *J. Biol. Chem.* **278**: 48210–48218.